0023-6837/01/8110-1457$03.00/0
LABORATORY INVESTIGATION
Vol. 81, No. 10, p. 1457, 2001

Printed in U.S.A.

Sequential Multilocus Fluorescence In Situ Hybridization Can Detect Complex Patterns of Increased Gene Dosage at the Single Cell Level in Tissue Sections

Axel Walch, Karin Bink, Peter Hutzler, Katharina Böwering, Ioanna Letsiou, Horst Zitzelsberger, Herbert Braselmann, Hubert Stein, Heinz Höfler, and Martin Werner

Institute of Pathology (AW, KBi, KBö, IL, HH), Technische Universität München, Munich; Institute of Pathology (AW, KBi, PH, HH, MW) and Institute of Radiation Biology ((HZ, HB), GSF-National Research Center for Environment and Health, Neuherberg; and Department of Surgery (HS), Technische Universität München, Munich, Germany

Although some impressive applications of multicolor fluorescence in situ hybridization (M-FISH) have been demonstrated on cytogenetic preparations, there are no reports of studies that carry over these advanced multitarget techniques to histological sections of tumor tissues in molecular pathology. Despite recent advances in protocols, M-FISH with a simultaneous multicolor painting tool does not seem to be a feasible approach in histological sections, mainly because of the inherent problem of the third dimension, which leads to complex overlays of both fluorescence signals and nuclei of tumor cells. To overcome these technical limitations, we introduce here an innovative and robust method for the detection of multiple targets by interphase FISH in formalin-fixed and paraffin-embedded tissue, called sequential multilocus fluorescence in situ hybridization (SML-FISH).

Each single tissue section (10 μm) obtained from two different paraffin blocks of formalin-fixed tissue from a surgical resection specimen of primary adenocarcinoma of distal esophagus (Union Internationale Contre le Cancer [UICC] Classification: pT1, pN0, pM0; Graduation: G2) was mounted on a glass slide. Tissue pretreatment was done by heating the slides for 20 minutes in a microwave oven (750 W); additionally, pronase E (0.05%) digestion for 10 minutes was performed. Denaturation was performed as described elsewhere (Werner et al, 1999). The following commercially available fluorescent-labeled, locus-specific (LSI), and associated centromere DNA probes (CEP) (Vysis, Inc., Downers Grove, Illinois) were sequentially applied according to manufacturers' instructions in the listed order: LSI D7S486 (c-met), CEP 7, LSI c-myc, CEP 8, LSI Cyclin D1, CEP 11, LSI Her-2/*neu*, CEP 17, LSI 20q13.2, and CEP 20. After hybridization of the first probe (LSI D7S486), the slides were placed in $\times$2 SSC, 0.1% NP-40 (pH 7.4) at 73° C for 2 minutes followed by embedding with an antifade solution (Vysis, Inc.) containing 4',6-diamidino-2-phenylindole (DAPI) as nuclear counterstaining. Three-dimensional volume data sets for the corresponding fluorescence channel (DNA probe and nuclear counterstaining) were generated using a confocal laser scanning microscope (CLSM, Zeiss LSM 510; Carl Zeiss, Jena, Germany). For these purposes each area was scanned in high resolution mode (lens PNF 40$\times$/1.3 Oil; scaling X = Y = 0.22 μm, Z = 0.5 μm) resulting in an image stack of DNA probes and nuclear counterstaining of each tumor area. After image aquisition, the first DNA probe (LSI D7S486) was washed out by heating the section in $\times$2 SSC at 73° C for 25 minutes, followed by denaturation at 73° C for 5 minutes in 70% formamide/$\times$2 SSC. After deletion of the DNA probe which followed after the laser scanning procedure before the next hybridization, the section was evaluated to ensure that there were no DNA probe-specific fluorescent signals left. Then, the procedure (hybridization, nuclear counterstaining, image aquisition of the same tissue areas, and deletion of the probe) was repeated for each of the remaining probes. Signal evaluation was performed by use of the various visualization techniques of the Zeiss LSM Image Browser, Version 2.80.1123. To avoid misinterpretation resulting from insufficient hybridization, cells were counted only if at least one bright specific signal was present. Signal interpretation, referred to as high-level gene amplification, low-level gene amplification, and chromosomal polysomy, was performed as previously published (Sauter et al, 1996).

Received June 6, 2001.
This work was supported by Bayerische Forschungsstiftung.
Address reprint requests to:
Dr. Axel Walch, Institut für Allgemeine Pathologie und Pathologische Anatomie, Ismaninger Straße 22, D-81675 München, Germany. E-mail: axel.walch@lrz.tum.de

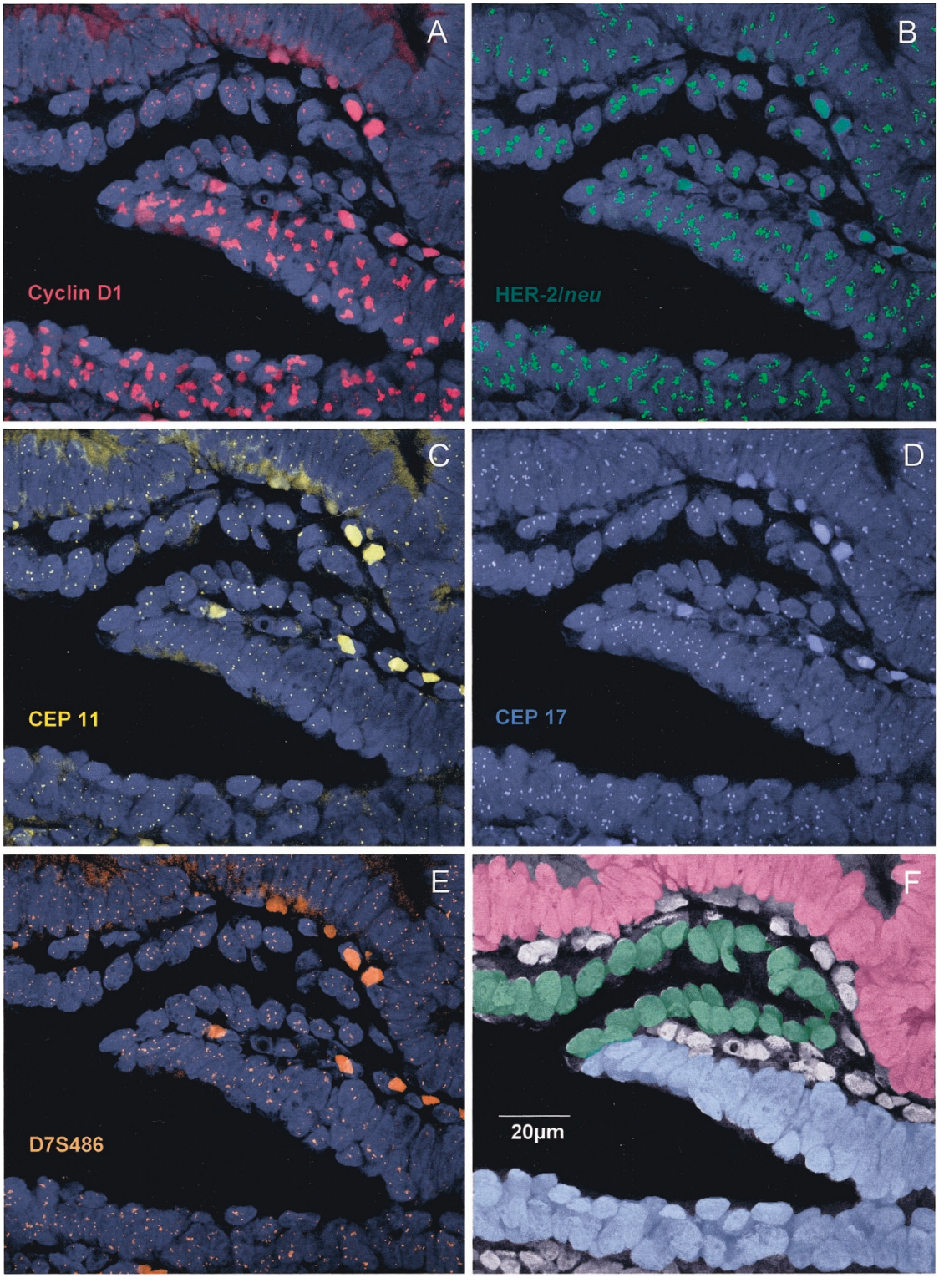

Figure 1.

Projections (two dimensional) of confocal image stacks of the same cells (counterstained with 4',6-diamidino-2-phenylindole [DAPI], displayed in gray) within a tumor area of Barrett's adenocarcinoma. The fluorescent-labeled DNA probes are specific for cyclin D1 (A, red signals), HER-2/*neu* (B, green signals), centromere 11 (C, yellow signals), centromere 17 (D, blue signals), and D7S486 (E, orange signals). A comparative analysis of changes in individual tumor cells, schematically shown in Panel F, allows the identification of distinct cell populations characterized by a specific pattern of changes. These cells, which are indicated by the blue color (F), are characterized by co-amplification of HER-2/*neu* (B) and cyclin D1 (A), both with clusters representing high-level amplification. Additionally, some of these nuclei display polysomy #11 and #17, whereas other present disomic counts. The signal number of D7S486 is also slightly elevated (E). In contrast, those cells indicated by the green color merely display high-level amplification of HER-2/*neu* (B), whereas cyclin D1 (A) shows increased signals (ie, polysomy), and additionally, polysomy #11 and #17 is present (C and D). The cell population, indicated in red, shows disomic counts for cyclin D1 and centromere 11, whereas amplification of HER-2/*neu* is present. Note, there are no changes in the nuclei of stromal cells (lymphocytes and fibrocytes, white nuclei in Panel F) in the immediate surroundings of tumor cells.

Complex patterns of increased gene dosage for c-met, c-myc, cyclin D1, Her-2/*neu*, and 20q13.2, as well as different levels of aneuploidy for associated chromosomes 7, 8, 11, 17, and 20, were found at the single-cell level in situ (Fig. 1, A to E). Amplification of LSI Her-2/*neu* was detected homogeneously as signal clusters in almost every tumor cell investigated in both samples (Fig. 1B). In contrast, LSI cyclin D1 displayed a strikingly heterogeneous pattern ranging from tumor cells with a disomy to those displaying high-level amplification in Sample 1 (Fig. 1A), whereas tumor cells in Sample 2 showed no amplification for LSI cyclin D1 (data not shown). Although the majority of tumor cells displayed no amplification for LSI D7S486 (c-met), LSI c-myc, and LSI 20q13.2, individual cells were observed showing increased signal numbers up to 10 signals per nucleus for these LSI probes. Coamplification of LSI Her-2/*neu* and LSI Cyclin D1 was most striking in approximately one-third of tumor cells within Sample 1 (Fig. 1, A and B). The observed signal number of CEP 7, CEP 8, and CEP 20 indicated polysomy #7, #8, and #20 present at different degrees within the tumor cells, whereas CEP 11 and CEP 17 also displayed areas with disomic counts. There was a correlation between LSI c-myc and LSI cyclin D1 (Pearson $p < 0.10$, Spearman $p < 0.005$) present as increased copy numbers of c-myc (ie, polysomy) in all cells showing LSI cyclin D1 clusters (ie, high-level amplification). Furthermore, correlations between LSI D7S486 (c-met) and LSI 20q13.2 (Pearson $p = 0.0096$, Spearman $p = 0.015$; Sample 1) and CEP 11 and CEP 17 (Pearson $p < 0.005$, Spearman $p < 0.05$; Samples 1 and 2) could be demonstrated. The strongest correlation between LSI/CEP pairs was found for CEP 7 and LSI D7S486 (Pearson $p < 0.001$, Spearman $p < 0.001$). Thus, the application of SML-FISH on tissue sections opens an unique insight into complex molecular genetic events in situ. We illustrate this powerful approach by applying SML-FISH to Barrett's adenocarcinoma, which is previously presumed to exhibit intratumoral heterogeneity as indicated by PCR-based experiments (Barrett et al, 1999; Galipeau et al, 1996). Instead of generalized polyploidization or gene amplification, we could demonstrate different levels of chromosomal polysomy in combination with changing patterns of distinct locus-specific copy number changes within and between individual tumor cells. Thus, the intratumoral heterogeneity in situ in the present case was much more extensive than previously expected.

An important reason for the application of a sequential (SML-FISH) instead of a simultaneous approach (M-FISH) is the inherent problem of the third dimension in tissue sections. The limited three-dimensional optical resolution can result in complex signal overlays, and proper segmentation of signals in the overlapping nuclei, which is a prerequisite for the image-analysis procedures of M-FISH, is still an unsolved problem. In addition, a simultaneous approach applying multiple DNA probes might be hampered by the presence of hundreds of signals in case of coamplification of multiple genes. Such a plethora of fluorescent signals in single cells would also result in complex signal overlays, even if laser scanning microscopy were applied. Whereas M-FISH requires sophisticated DNA probe designing and large-scale technical equipment to differentiate the colors and, therefore, unequivocally distinguish the origin of every target in a hybridized cell, SML-FISH is much more robust and can be performed with all kinds of commonly available fluorescent-labeled DNA probes.

References

Barrett MT, Sanchez CA, Prevo LJ, Wong DJ, Galipeau PC, Paulson TG, Rabinovitch PS, and Reid BJ (1999). Evolution of neoplastic cell lineages in Barrett oesophagus. Nat Genet 22:106–109.

Galipeau PC, Cowan DS, Sanchez CA, Barrett MT, Emond MJ, Levine DS, Rabinovitch PS, and Reid BJ (1996). 17p (p53) allelic losses, 4N (G2/tetraploid) populations, and progression to aneuploidy in Barrett's esophagus. Proc Natl Acad Sci USA 93:7081–7084.

Sauter G, Feichter G, Torhorst J, Moch H, Novotna H, Wagner U, Durmuller U, and Waldman FM (1996). Fluorescence in situ hybridization for detecting erbB-2 amplification in breast tumor fine needle aspiration biopsies. Acta Cytol 40:164–173.

Werner A, Mattis M, Aubele M, Cummings C, Zitzelsberger H, Hutzler P, and Hofler H (1999). 20q13.2 amplification in intraductal hyperplasia adjacent to in situ and invasive ductal carcinoma of the breast. Virchows Arch 435:469–472.